SAND2020-13312C

Nonlinear characteristics of cantilevered pipelines conveying fluid with multi-segmented motion limiting constraints

Timothy Alvis[1], Abdessattar Abdelkefi[2]

Abstract

Advancements in the development and understanding of the nonlinear dynamics of cantilevered pipes conveying fluid have been made over many decades. Although the applications of cantilevered pipes conveying fluid seem to be simple, researchers have continued to modify the system to study the interesting linear and nonlinear responses. In this study, the equations of motion of a modified system with multisegmented motion limiting constraints are derived and discretized using the Galerkin method. The response of the system with multi-segmented motion limiting is studied by investigating the bifurcation diagrams of the system with different constraint stiffnesses. Various kinds of bifurcations are characterized depending on the stiffnesses of the multi-segmented force.

I. Introduction

Cantilevered pipelines conveying fluid have been implemented in many applications throughout history, such as pipelines and risers [1], mechanical pumps [2], and micro\nano-pipelines that could be used as drug delivery devices [3, 4]. Because of the wide variety of applications and the importance of understanding the dynamic responses and stability of these systems, many researchers have studied the linear and nonlinear dynamics of cantilevered pipelines conveying fluids for many years. To better characterize these systems, researchers have modified the system by implementing new parameters including a tip mass to the pipe, linear and nonlinear springs along the length of the pipe, and adding motion limiting constraints. The motion limiting constraints can better control the motion of the pipe, but it introduces an impact force which can cause various nonlinear responses, such as aperiodic and chaotic oscillations at sufficient flow speed, and grazing bifurcations which occurs when the oscillating pipe reaches one of the constraints tangentially with zero speed [5].

Motion limiting constraints were implemented by Païdoussis and his co-authors [6, 7]. In their studies, they focused on the nonlinear response of the system both experimentally and analytically. They assumed the motion of the pipe was occurring in one planar direction. To implement this into the experiments, a steel strip was embedded into the center of the pipe, as depicted in Figure 1.

[1]PhD student, Department of Mechanical and Aerospace Engineering, New Mexico State University, Las Cruces, NM 88003, USA.
[2]Associate Professor, Department of Mechanical and Aerospace Engineering, New Mexico State University, Las Cruces, NM 88003, USA.

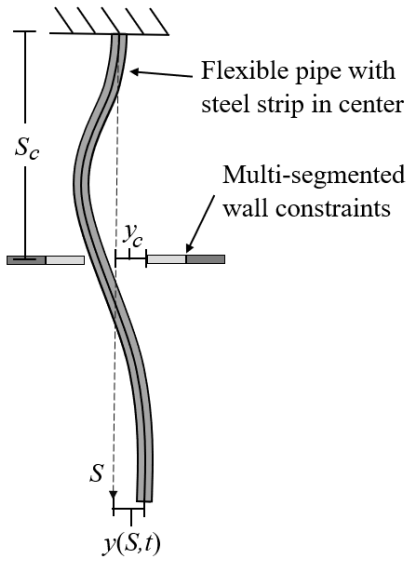

Figure 1. Schematic of pipeline with embedded steel strip for planar motion.

Although motion limiting constraints were implemented in previous studies [6, 7], it is interesting to consider the implementation of multi-segmented constraints with various stiffnesses. With the addition of these multi-segmented constraints, a better accuracy of the stoppers is introduced, and it is then possible to have a more desirable representation of this contact problem. It is important to note, however, that only the dynamic response at the tip of the pipe was deeply investigated. It is possible that grazing bifurcations, period doubling, and chaos could occur at different flow speeds at the point of contact compared to the tip. Taylor et al. [8] verified previous numerical and experimental results shown in at the tip of the pipe [6, 7] and expanded on it by comparing to the same key flow speed velocities at the point of contact. In [8], it was found that instances of chaotic behavior, sticking, and grazing bifurcations at the point of contact did not necessarily occur at the same flow speed at the tip. It was concluded that in the case of cantilevered pipelines conveying fluid with motion limiting constraints, more accurate responses can be described by characterizing the system at the point of contact [8].

In this study, using the extended Hamilton's principle, the full nonlinear equation of motion is derived while considering the multi-segmented constraints function. Then, the full nonlinear equation of motion is nondimensionalized and discretized using Galerkin's method. After that, using a Runge-Kutta based algorithm, the bifurcation diagrams are determined for various representations of the multi-segmented constraint.

II. System's reduced-order modeling

Equation (1) shows the expression of the multi-segmented motion limiting constraints.

$$f(y)=\begin{cases}\kappa_2 y+\kappa_1\delta_1+(\kappa_2-\kappa_1)\delta_2, & \text{if } y<-\delta 2\\ \kappa_1(y+\delta_1), & \text{if } -\delta_2<y<-\delta_1\\ 0, & \text{if } |y|<\delta_1\\ \kappa_1(y-\delta_1), & \text{if } \delta_2>y>\delta_1\\ \kappa_2 y+\kappa_1\delta_1+(\kappa_2-\kappa_1)\delta_2, & \text{if } y>\delta 2\end{cases} \quad (1)$$

where κ_1 and κ_2 are the stiffnesses of the inner and outer constraint respectively, y denotes the displacement of the pipe. To have the best understanding of how a true impact affects the output of the system, four different increasing stiffnesses are implemented for κ_2. The first stiffness is equal to the inner constraint's stiffness at $\kappa_1=\kappa_2=980$. The second stiffness is set to ten times the inner stiffness at $\kappa_2=9,800$. The third stiffness is set to twenty times the inner stiffness at $\kappa_2=19600$, and the final stiffness is one thousand times the inner stiffness at $\kappa_2=980,000$. This high stiffness value will give us a good understanding of how a system under a true impact behaves. Figure 2 shows the constraint force produced with multi-segmented constraints with the specified stiffnesses, and the two contacts are at $\delta_1=0.044$ and $\delta_2=0.066$.

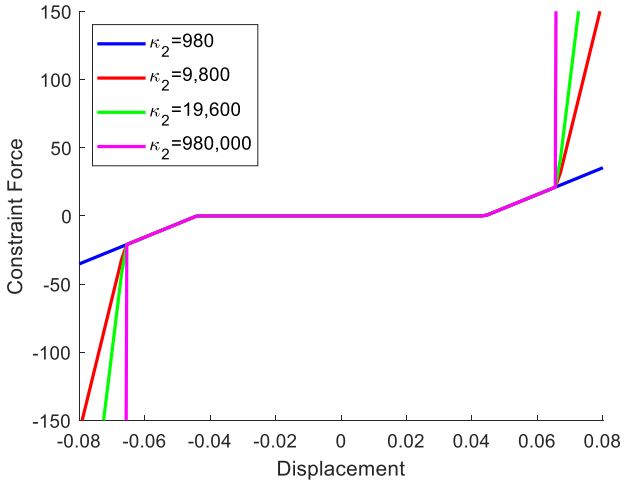

Figure 2. Forcing function estimating constraint forces for multi-segmented constraints.

To have a simple representation of the system under investigation and an inexpensive computational cost, a nonlinear reduced-order model is developed by making justified assumptions to neglect certain terms while maintaining the desired behaviors. Important assumptions to make with this study is that the pipe is inextensible, the fluid velocity is uniform, the fluid is incompressible, the deformation is large, but the strain is small; and the diameter of the pipe is much smaller than the length of pipe. Therefore, the Euler-Bernoulli beam theory can be applied. Knowing these assumptions and

by following the work of Semler et al. [9], the extended Hamilton's principle and the inextensibility condition can be implemented to find the fully nonlinear equation of motion as:

$$\begin{aligned}
&EI\left(y^{iv}+\eta\dot{y}^{iv}\right)+2MU\dot{y}'+MU^2y''-\left(m+M\right)g\left(L-s\right)y''+\left(m+M\right)\ddot{y}+2MU\dot{y}'y'^2\\
&+y''y'^2\left[MU^2-\frac{3}{2}\left(m+M\right)g\left(L-s\right)\right]+\frac{1}{2}g\left(m+M\right)y'y'^2+EI\left(y^{iv}y'^2+4y'''y''y'+y''^3\right)\\
&-y''\left[\int_s^L 2MUy'\dot{y}'+MU^2y'y''+\int_0^s\left(m+M\right)\left(\dot{y}'^2+y'\ddot{y}'\right)ds\,ds\right]+y'\int_0^s\left(m+M\right)\left(\dot{y}'^2+y'\ddot{y}'\right)ds\\
&+F\left(y\right)\delta\left(s-s_c\right)
\end{aligned} \tag{2}$$

where M represents the mass per unit length of the fluid, m is the mass per unit length of the pipe, L denotes the length of the pipe, s is the curvature, U represents the flow speed, η is the Kelvin-Voigt damping, and F denotes the force applied by the constraints. It is important to note that several nonlinearities are present from the inextensibility condition.

The governing equation is then nondimensionalized with the following relationships:

$$\begin{gathered}
s=\frac{s}{L},\ y=\frac{y}{L},\ \tau=\left(\frac{EI}{m+M}\right)^{\frac{1}{2}}\frac{t}{L^2},\ \xi=\left(\frac{EI}{m+M}\right)^{\frac{1}{2}}\frac{\eta}{L^2},\ u=\left(\frac{M}{EI}\right)^{\frac{1}{2}}UL,\ \gamma=\frac{m+M}{EI}L^3g,\\
m_r=\frac{M}{m+M},\ f\left(y\right)=\frac{F\left(y\right)L^3}{EI}
\end{gathered} \tag{4}$$

The nonlinear equation of motion is then expressed as follows [9]:

$$\begin{aligned}
&\ddot{y}+\xi\dot{y}^{iv}+2u\sqrt{m_r}\dot{y}'+y^{iv}+y''\left[u^2-\gamma\left(1-s\right)\right]+\gamma y'+2u\sqrt{m_r}\dot{y}'y'^2+y''y'^2\left[u^2-\frac{3}{2}\gamma\left(1-s\right)\right]\\
&+\left(-\frac{1}{2}\gamma y'^3+3y'''y''y'+y''^3\right)-y''\int_s^1\left(-\gamma y'^2+2u\sqrt{m_r}\dot{y}'y'+u^2y''y'+y'''y''\right)ds\\
&-y''\int_s^1\int_0^s\left[\dot{y}'^2-2u\sqrt{m_r}\dot{y}''y'-y'''y'\left(u^2\gamma\left(1-\xi\right)\right)+y^{iv}y''\right]dsds\\
&+y'\int_0^s\left[\dot{y}'^2-2u\sqrt{mr}\dot{y}''y'-y'''y'\left(u^2-\gamma\left(1-s\right)\right)+y^{iv}y''\right]ds+f\left(y\right)\delta\left(s-s_c\right)
\end{aligned} \tag{5}$$

After that, using the known cantilever beam mode shapes $\Phi_i(s)$, and the general modal coordinate $q_i(\tau)$, the Galerkin method is applied and simplified into a nonlinear reduced-order model as follows:

$$\begin{aligned}
&\ddot{q}_i+\left[C_{ij}+y\left(C_u\right)_{ij}\right]\dot{q}_j+\left[K_{ij}+u^2\left(K_u\right)_{ij}\right]q_j+\left[M_{ijkl}\right]\dot{q}_j\dot{q}_kq_l+\left[uN_{ijkl}\right]\dot{q}_jq_kq_l\\
&+\left[P_{ijkl}+u^2\left(Pu\right)_{ijkl}\right]q_jq_kq_l+f\left(\sum_{z=1}^{N}\Phi_z\left(s_b\right)q_z\left(\tau\right)\right)\Phi_i\left(s_b\right)
\end{aligned} \tag{6}$$

III. Results

The nonlinear reduced-order model is then analyzed, and bifurcation diagrams are produced. The bifurcation diagram shows the oscillation of the pipe. Each point on the diagram represents a local/global peak value in the time history of the system's oscillation. This allows researchers to understand how the behavior changes as the pipe moves. The bifurcation diagram for each stiffness is shown in Figure 3. It should be mentioned that only some preliminary results are shown in this study.

It follows from the plotted curves in Figure 3 that as the system starts conveying fluid, it remains still and does not oscillate. However, once a critical internal flow speed is reached, the system starts oscillating. Then, for all considered configurations, it is clear that the onset of Hopf bifurcation is independent of the constraint and a supercritical Hopf bifurcation takes place. The dashed black lines in Figure 3 show where the behavior of the pipe changes and the blue dotted lines show the locations of the boundaries of each stiffness. Inspecting the plots in Figure 3, it can be noted that the pipe oscillates periodically near Hopf bifurcation, but once the pipe strikes the first constraint, the pipe has aperiodic responses around the two constraint locations. This aperiodic response may be due to a grazing bifurcation which occurs when the pipe comes into the contact with the constraint tangentially at zero velocity. This behavior continues for a time, but eventually, the system begins to oscillate periodically again, although, it is no longer centered around its original position. Then, the pipe contacts the second constraint. As expected, the four systems behave the same until the pipe contacts the outer constraint. This is because the inner constraint stiffness and other initial conditions remain the same between each case. It is also clear that the system behaves as if there is only one constraint in Figure 3(a) because the stiffness of the outer constraint is equal to the stiffness of the inner constraint.

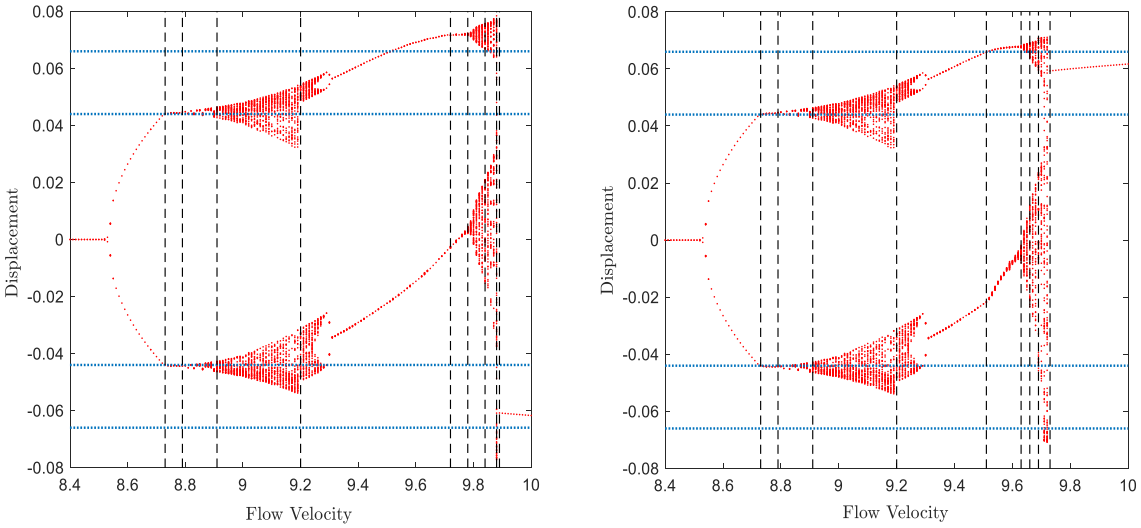

(a) (b)

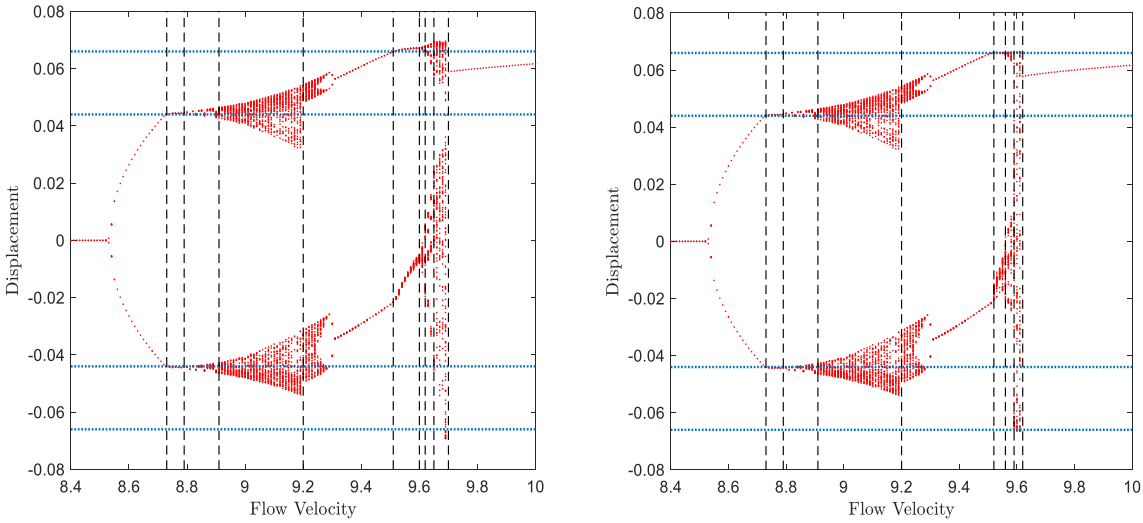

(c) (d)

Fig. 3 Bifurcation diagrams at point of contact where (a) $\kappa_1 = \kappa_2 = 980$, (b) $\kappa_2 = 9,800$, (c) $\kappa_2 = 19,600$, and (d) $\kappa_2 = 980,000$.

A deep investigation is performed when the pipe contacts the second constraint, as shown in Figure 4. One behavior of note is that at a certain flow speed, the pipe begins to stick to one wall or the other and no longer oscillates. In Figure 4(a), the pipe sticks in the wall on the negative axis, where the other three pipes stick to the positive axis constraint. By increasing the stiffness of the outer constraint, the flow speed to reach sticking lowers. This behavior is expected as the stiffness of the constraints increase. The values for the flow speed at sticking for each stiffness are listed in Table 1. It is clear that as the outer constraint stiffness is increased, all behavior is shifted towards lower flow speeds. By looking at Figures 4(a-c), the pipe travels into the second constraint, but it does not at the highest stiffness value. When the pipe is displacing into these constraints, it is possible that a new bifurcation is occurring called grazing-sliding bifurcation. This is like the grazing bifurcation mentioned earlier, but in grazing sliding bifurcation the pipe meets the constraint tangentially at zero velocity and slides along the wall for a time. This is the beginning of the pipe sticking to the constraint. More investigations are needed by studying the pipe's time histories, phase portraits, and Poincare maps. Indeed, time histories and Poincare maps will be developed for each bifurcation diagram before and after each behavior change to gain a better understanding of the system's response and to characterize the different bifurcations. Additionally, the stiffness of the first constraint will be investigated. Once a group of stiffnesses has been selected for each constraint, different combinations of stiffnesses will be analyzed to determine which pairing has the most positive effect.

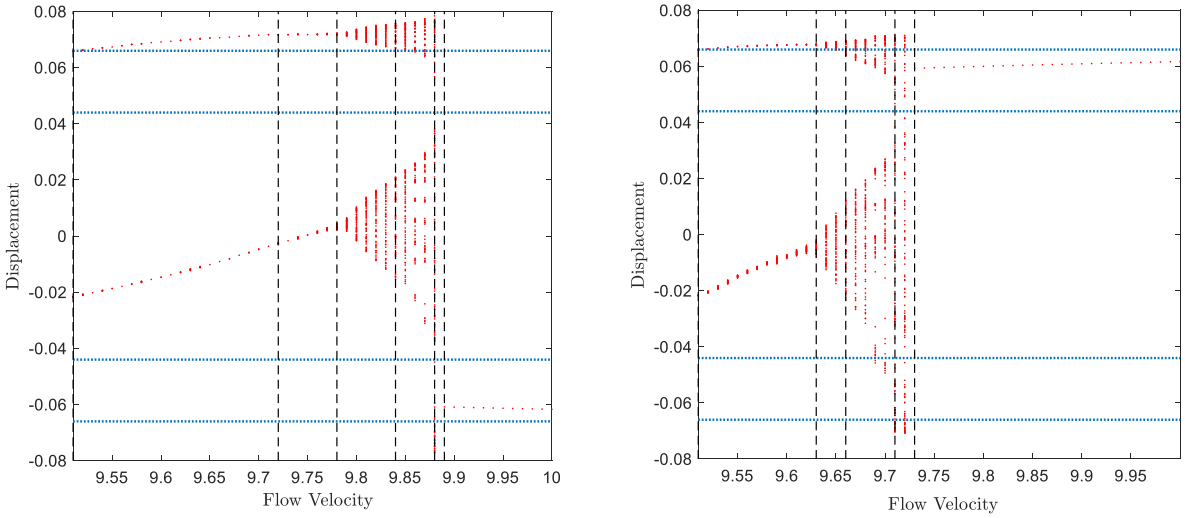

(a)

(b)

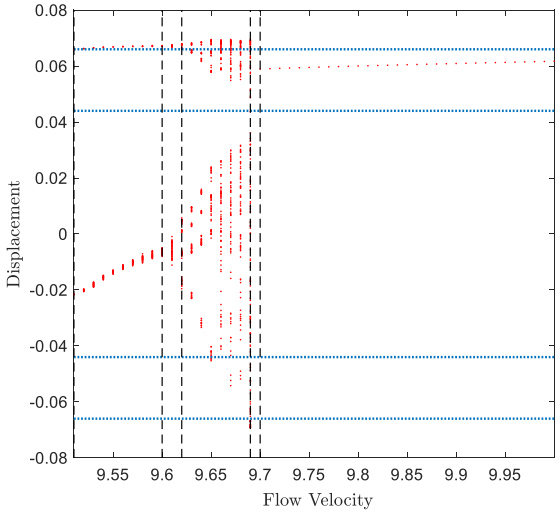

(c)

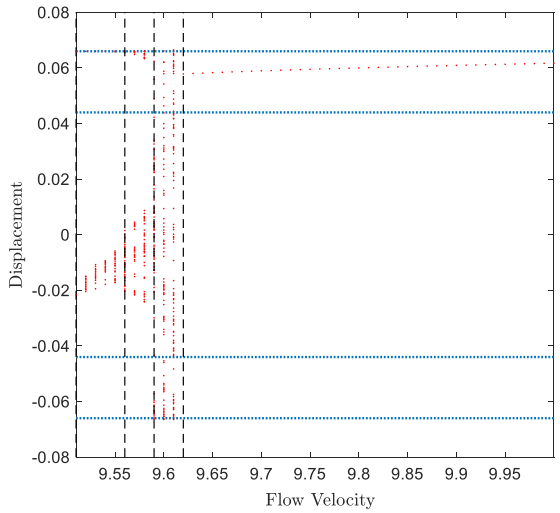

(d)

Fig. 4 Bifurcation diagrams at point of contact zoomed in to show where the pipe contacts the outer constraint where (a) $\kappa_1 = \kappa_2 = 980$, (b) $\kappa_2 = 9{,}800$, (c) $\kappa_2 = 19{,}600$, and (d) $\kappa_2 = 980{,}000$.

Table 1. Internal flow speed at which sticking occurs for each outer constraint stiffness investigated.

	Flow speed at sticking
$\kappa_2 = 980$	9.89
$\kappa_2 = 9{,}800$	9.73
$\kappa_2 = 19{,}600$	9.7
$\kappa_2 = 980{,}000$	9.62

IV. Conclusions

An understanding of the linear and nonlinear dynamics of cantilevered pipelines conveying fluid is essential because of the wide variety of important applications. Researchers have been studying these systems for decades, with each new researcher modifying the system in a new way that helps better the common understanding of the dynamic and chaotic behaviors these systems can induce. Previous researchers have found a way to assist in controlling the pipeline by adding motion limiting constraints, but these constraints can cause chaotic behaviors from grazing bifurcations and others. This work developed the use of multi-segmented motion limiting constraints and showed that the result of increasing the stiffness of the outer constraint decreases the critical flow speed at which sticking occurs. This decreases the overall period of chaotic behavior and might be useful to future engineers while designing these pipeline systems.

Acknowledgments

The authors would like to thank the financial support from Sandia National Laboratories.

This paper describes objective technical results and analysis. Any subjective views or opinions that might be expressed in the paper do not necessarily represent the views of the U.S. Department of Energy or the United States Government.

The authors would like to thank Gregory Taylor for his assistance with developing the modeling of the system and continued support throughout this research.

References

[1] Housner, G. W., "Bending vibrations of a pipe when liquid flows through it," *Journal of Applied Mechanics,* vol. 19, pp. 205-208, 1952.

[2] Askarian, A. R. , Haddapour, H., Firouz-Abadi, R., Abtahi, H., "Nonlinear dynamics of extensible viscoelastic cantilevered pepes converying pulsatile flow with an end nozzle," *Internationsl Journal of Non-Linear Mechanics,* vol. 91, pp. 22-35, 2017.

[3] Wang, L., Hong, Y., Dai, H., Ni, Q., "Natural frequency and stability tuning of cantilebered CNTs conveying fluid in magnetic field," *Acta Mechanica Solida Sinica,* vol. 29, pp. 567-576, 2016.

[4] Rinaldi, S. , Prabhakar, S., Vengallator, S., Paidoussis, M., "Dynamics of microscale pipes containting internal fluid flow: damping, frequency shift, and stability," *Journal of Sound and Vibration,* vol. 329, pp. 1081-1088, 2010.

[5] Whiston, G., "Global dynamics of vibro-impacting linear oscillator," *Journal of Sound and Vibration,* vol. 118, pp. 395-424, 1987.

[6] Paidoussis, M. P., Semler, C. "Nonlinear and chaotic oscillations of a constrained cantilevered pipe conveying fluid: a full nonlinear analysis," *Nonlinear Dynamics,* vol. 4, pp. 655-670, 1993.

[7] Paidoussis, M. P., Li, G. X., Rand, R. H., "Chaotic motions of a constrained pipe conveying fluid: comparison between simulation, analysis, and experiment," *Jounal of Applied Mechanics,* vol. 58, pp. 559-565, 1991.

[8] Taylor, G., Ceballes, S., Abdelkefi, A., "Insights on the point of contact analysis and characterization of constrained pipelines conveying fluid," *Nonlinear Dynamics,* vol. 93, pp. 1261-1275, 2018.

[9] Semler, C., G. Li, X., Paidoussis, M. P., "The non-linear equations of motion of pipes conveying fluid," *Jounral of Sound and Vibration,* vol. 169, no. 5, pp. 577-599, 1994.